J|A|C|S
ARTICLES
Published on Web 07/11/2006

Chiral Three-Dimensional Microporous Nickel Aspartate with Extended Ni−O−Ni Bonding

Ekaterina V. Anokhina,[†] Yong Bok Go,[†] Yongjae Lee,[‡,§] Thomas Vogt,[‡,||] and Allan J. Jacobson*[,†]

Department of Chemistry, University of Houston, Houston, Texas 77204 and Physics Department, Brookhaven National Laboratory, Upton, New York 11973

Received April 19, 2006; E-mail: ajjacob@uh.edu

Abstract: In the course of our investigation aimed at the preparation of homochiral coordination polymers using readily available in optically pure form ligands and building blocks of condensed metal polyhedra, we recently reported a one-dimensional nickel aspartate compound $[Ni_2O(L\text{-}Asp)(H_2O)_2]\cdot 4H_2O$ (**1**) based on helical chains with extended Ni−O−Ni bonding. Here we report a new nickel aspartate $[Ni_{2.5}(OH)(L\text{-}Asp)_2]\cdot 6.55H_2O$ (**2**) with a three-dimensional Ni−O−Ni connectivity that forms at a higher pH and is based on the same helices as in **1** which are connected by additional nickel octahedra to generate a chiral open framework with one-dimensional channels with minimum van der Waals dimensions of 8 × 5 Å. The crystal structure of **2** was determined by synchrotron single-crystal X-ray diffraction on a 10 × 10 × 240 μm crystal.

Introduction

Increasing demand for materials for enantioselective catalysis and separation[1] and interest in fundamental aspects of chirality and molecular recognition[2] have stimulated extensive research in the area of chiral coordination polymers.[3] While optically pure single crystals can occasionally result from achiral starting materials due to spontaneous resolution, the main synthetic strategy to induce chirality and prepare an enantiomerically pure bulk material has been the use of pre-resolved chiral multidentate ligands. Chiral ligands naturally occurring in a pure enantiomeric form and their derivatives have received significant attention since, while lacking the predictability of network topology recently achieved with "designer" synthetic ligands,[4] they are readily available and do not require complex synthesis and chiral resolution procedures.[5] For example, a chiral ligand derived from tartaric acid led to a layered zinc compound "POST-1" that has triangular chiral channels (side length of a triangle 13.4 Å) and enantioselectively absorbs transition-metal complexes.[6] A carboxylic derivative of quinine formed a three-dimensional coordination polymer with cadmium that enantioselectively absorbs (*S*)-2-butanol and (*S*)-2-methyl-1-butanol.[5a] A zinc saccharate three-dimensional coordination polymer $[Zn(C_6H_8O_8)]\cdot 2H_2O$ features two types of channels, hydrophilic and hydrophobic (5.8 × 5.8 Å), and can absorb molecules such as azobenzene.[7] Natural amino acids are also well known to form coordination polymers with transition metals (TM), although the main focus of the extensive studies on amino acid coordination chemistry has been on their biologically relevant molecular complexes. For example, Ni^{2+}, Co^{2+}, Mn^{2+}, and Zn^{2+} form aspartates $[MAsp(H_2O)_2]\cdot H_2O$[8] that are based on one-dimensional helical chains, and Co^{2+}, Cu^{2+}, Cd^{2+}, and Zn^{2+} form three-dimensional glutamates $[MGlu(H_2O)]\cdot H_2O$.[9] The vast majority of chiral coordination polymers are based on mononuclear metal centers. Condensation of metal polyhedra into oligomeric units or extended arrays in hybrid frameworks with achiral ligands has led to numerous examples of materials with remarkable structural and physical properties.[10] Among them especially notable are nickel succinate $[Ni_7(OH)_2(C_4H_4O_4)_6(H_2O)_2]\cdot 2H_2O$[11] and nickel glutarate $[Ni_5\{(C_5H_6O_4)_5(H_2O)_2\}]\cdot$

[†] University of Houston.
[‡] Brookhaven National Laboratory.
[§] Current address: Department of Earth System Sciences, Yonsei University, Seoul 120749, Korea.
[||] Current address: Department of Chemistry and Biochemistry, The University of South Carolina, Columbia, South Carolina 29208.

(1) (a) Maier, N. M.; Franco, P.; Lindner, W. *J. Chromatogr. A* **2001**, *906*, 3. (b) Baiker, A. *Curr. Opin. Solid State Mater. Sci.* **1998**, *3*, 86. (c) Song, C. E.; Lee, S. G. *Chem. Rev.* **2002**, *102*, 3495.
(2) In *Chirality in Natural and Applied Science;* Lough, W. J., Wainer, I. W., Eds.; CRC Press: Boca Raton, 2002.
(3) (a) Kesanli, B.; Lin, W. *Coord. Chem. Rev.* **2003**, *246*, 305. (b) Janiak, C. *Dalton Trans.* **2003**, 2781 and references therein.
(4) (a) Cui, Y.; Ngo, H. L.; Lin, W. *Chem. Commun.* **2003**, 1338. (b) Pschirer, N. G.; Ciurtin, D. M.; Smith, M. D.; Bunz, U. H. F.; zur Loye, H. C. *Angew. Chem., Int. Ed.* **2002**, *41*, 583.
(5) (a) Xiong, R.-G.; You, X.-Z.; Abrahams, B. F.; Xue, Z.; Che, C.-M. *Angew. Chem., Int. Ed.* **2001**, *40*, 4422. (b) Ranford, J. D.; Vittal, J. J.; Wu, D.; Yang, X. *Angew. Chem., Int. Ed. Engl.* **1999**, *38*, 3498. (c) Niklas, N.; Hampel, F.; Alsfasser, R. *Chem. Commun.* **2003**, 1586. (d) Wu, C.-D.; Lu, C.-Z.; Lin, X.; Wu, D.-M.; Lu, S.-F.; Zhuang, H.-H.; Huang, J.-S. *Chem. Commun.* **2003**, 1284.
(6) Seo, J. S.; Whang, D.; Lee, H.; Jun, S. I.; Oh, J.; Jeon, Y. J.; Kim, K. *Nature* **2000**, *404*, 982.
(7) Abrahams, B. F.; Moylan, M.; Orchard, S. D.; Robson, R. *Angew. Chem., Int. Ed.* **2003**, *42*, 1848.
(8) (a) Antolini, L.; Menabue, L.; Pellacani, G. C.; Marcotrigiano, G. *Dalton Trans.* **1982**, 2541. (b) Schmidbaur, H.; Bach, I.; Riede, J.; Muller, G.; Helbig, J.; Hopf, G. *Chem. Ber.* **1988**, *121*, 795. (c) Doyne, T. H.; Pepinsky, R.; Watanabe, T. *Acta Crystallogr.* **1957**, *10*, 438. (d) Kryger, L.; Rasmussen, S. E. *Acta Chem. Scan.* **1973**, *27*, 2674.
(9) (a) Zhang, Y.; Saha, M. K.; Bernal, I. *Cryst. Eng. Commun.* **2003**, *5*, 34. (b) Mizutani, M.; Maejima, N.; Jitsukawa, K.; Masuda, H.; Einaga, H. *Inorg. Chim. Acta* **1998**, *283*, 105. (c) Flook, R. J.; Freeman, H. C.; Scudder, M. L. *Acta Crystallogr., Sect. B* **1977**, *33*, 801. (d) Gramaccioli, C. M. *Acta Crystallogr.* **1966**, *21*, 600.

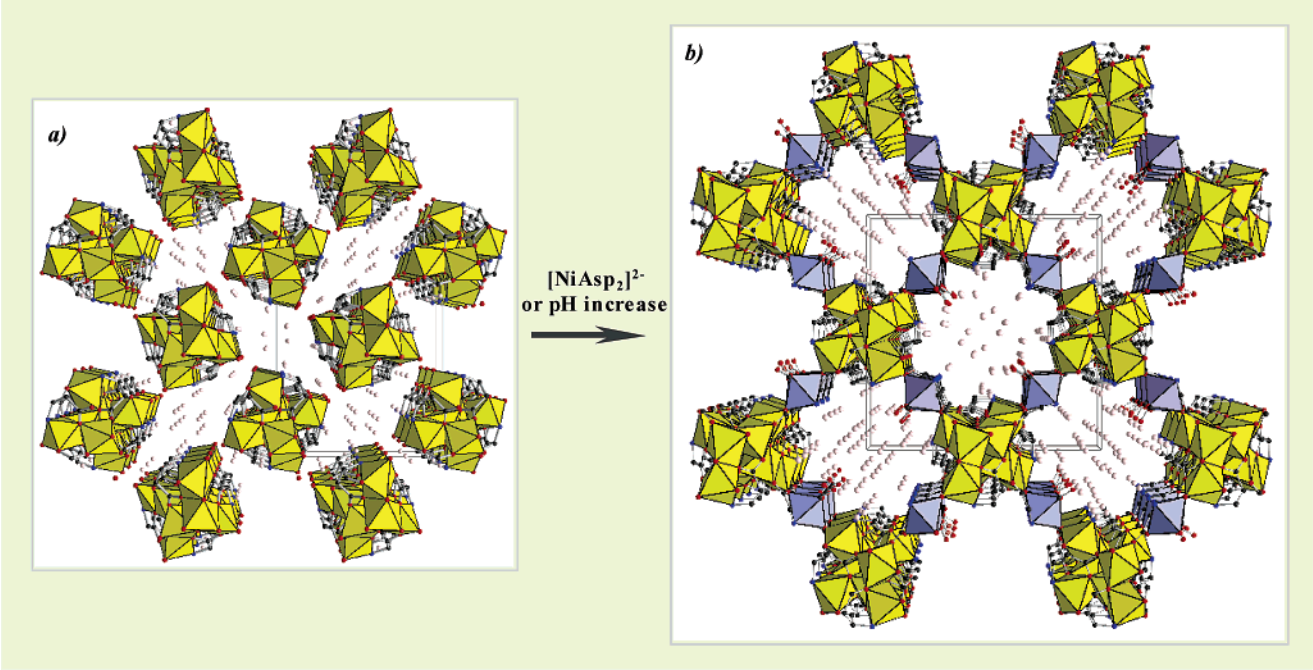

Figure 1. Crystal structures of (a) one-dimensional nickel aspartate $[Ni_2O(L\text{-}Asp)(H_2O)_2]\cdot 4H_2O$[14] (**1**) and (b) the title three-dimensional material $[Ni_{2.5}(OH)(L\text{-}Asp)_2]\cdot 6.55H_2O$ (**2**) that is formed by connecting chains in **1** through $[NiAsp_2]^{2-}$ bridges (shown as blue octahedra).

$8H_2O$[12] which have microporous rhombohedral and cubic frameworks, respectively, with a three-dimensional Ni−O−Ni connectivity. The nickel glutarate compound is chiral; however, due to the achiral nature of the glutarate ligand, the bulk product is racemic. These examples motivated us to investigate chiral amino acid−TM systems under synthesis conditions favoring hydrolysis of cations and formation of M−O-M bonding, i.e., elevated pH and mild hydrothermal conditions.[13]

We recently reported a one-dimensional nickel aspartate compound $[Ni_2O(L\text{-}Asp)(H_2O)_2]\cdot 4H_2O$ (**1**) composed of helical chains (11.6 Å in diameter) with extended Ni−O−Ni bonding (Figure 1a).[14] Here we present the structure and properties of a new three-dimensional nickel aspartate $[Ni_{2.5}(OH)(L\text{-}Asp)_2]\cdot 6.55H_2O$ (**2**) (Figure 1b) that forms at a higher pH and is based on analogous helices that are connected by additional nickel octahedra to generate a chiral open framework with one-dimensional channels with minimum van der Waals dimensions of 8 × 5 Å.

Experimental Section

Synthesis. *Optimized Conditions for the Synthesis of 2.* Compound **2** forms as a single-phase, light-blue powder under hydrothermal conditions from a reaction of stoichiometric amounts of $NiCl_2$ and L-H_2-Asp with the addition of Et_3N base. A 2.5 mL amount of a 2 M solution of $NiCl_2$, 2.0 mL of a 2 M solution of (Et_3NH)(L-HAsp), and 0.83 mL of Et_3N ($NiCl_2$:H_2Asp:Et_3N molar ratio of 1.25:1:2.5) were thoroughly mixed in a closed container, transferred to a 23 mL Teflon-lined autoclave, and heated at 150 °C for 4 days. The final pH of the mixture was 7.3. The product (70% yield based on Ni) was washed with distilled water and dried in air. Anal. Calcd for $C_8H_{24.10}N_2Ni_{2.5}O_{15.55}$: Ni, 26.98; C, 17.66; N, 5.15; H, 4.47. Found: Ni, 26.96; C, 17.67; N, 5.14; H, 4.38. The phase purity of the product was verified by powder diffraction, and the optical purity was confirmed by optical rotation measurements of a solution of **2** in 2 M HCl using a Jasco P-1010 polarimeter. The observed optical rotation value was the same as that of a reference solution of the corresponding amounts of $NiCl_2\cdot 6H_2O$ and L-H_2Asp in 2 M HCl. Scaling up this synthesis to 70 mL of the total volume of the initial mixture and carrying out the reaction in a 120 mL Teflon-lined autoclave also produced pure **2** in ca. 70% yield. Mixtures with the same $NiCl_2$:H_2Asp ratio but lower or higher amounts of the Et_3N base ($NiCl_2$:H_2Asp:Et_3N ratios of 1.25:1:2.25 and 1.25:1:2.75) led to impurities of $[NiAsp(H_2O)_2]\cdot H_2O$ and $Ni(OH)_2$, respectively. A reaction starting with a racemic (Et_3NH)(D,L-HAsp) solution led to conglomerate crystallization of L-**2** and D-**2**.

Crystal Growth of 2. The 1.25:1:2.5 mixture of $NiCl_2$, H_2Asp, and Et_3N initially forms a blue precipitate containing $[NiAsp(H_2O)_2]\cdot H_2O$ and $Ni(OH)_2$, which causes formation of a large number of nuclei and prevents growth of sizable crystals of **2** (average size 10.6 μm). A mixture of a 2 M solution of $NiCl_2$, a 2 M solution of (Et_3NH)(L-HAsp), and Et_3N ($NiCl_2$:H_2Asp:Et_3N molar ratio of 1:1:2, $pH_{ini} = 6.5$), on the other hand, initially remains as a clear solution and subsequently starts forming large (up to 2 × 2 × 2 mm) octahedral or prism-shaped blue crystals of $[NiAsp(H_2O)_2]\cdot H_2O$ which, upon heating above 140 °C, begin to transform to thin needles of **2** (formation of **2** from the mother liquor solution rather than from $[NiAsp(H_2O)_2]\cdot H_2O$ crystals was ruled out by the fact that heating a filtered mother liquor solution at 150 and 180 °C did not produce **2**). A pure sample of **2** could be separated from the $[NiAsp(H_2O)_2]\cdot H_2O$ crystals based on their different sedimentation rates from a suspension in ethanol. The largest crystals of **2** (0.010 × 0.010 × 0.24 mm) were obtained using the same ratio of the starting reagents (1:1:2) but increasing the concentration of the initial $NiCl_2$ solution from 2 M to 4 M. This mixture initially forms a blue solution with a small amount of oil-like blue precipitate that is soluble in water. This solution was centrifuged, transferred into a small brand-new glass container, which was placed into a Teflon-lined

(10) (a) Forster, P. M.; Cheetham, A. K. *Top. Catal.* **2003**, *24*, 79. (b) Hagrman, P. J.; Finn, R. C.; Zubieta, J. *Solid State Sci.* **2001**, *3*, 745. (c) Hagrman, P. J.; Hagrman, D.; Zubieta, J. *Angew. Chem., Int. Ed. Engl.* **1999**, *38*, 2638. (d) Yaghi, O. M.; O'Keeffe, M.; Ockwig, N. W.; Chae, H. K.; Eddaoudi, M.; Kim, J. *Nature* **2003**, *423*, 705. (e) Huang, Z. L.; Drillon, M.; Masciocchi, N.; Sironi, A.; Zhao, J. T.; Rabu, P.; Panissod, P. *Chem. Mater.* **2000**, *12*, 2805. (f) Lin, B.-Z.; Liu, S.-X. *Dalton Trans.* **2002**, 865.
(11) (a) Forster, P. M.; Cheetham, A. K. *Angew. Chem., Int. Ed.* **2002**, *41*, 457.
(12) Guillou, N.; Livage, C.; Drillon, M.; Férey, G. *Angew. Chem., Int. Ed.* **2003**, *42*, 5314.
(13) (a) Baes C. F.; Mesmer, R. E. *Hydrolysis of Cations;* Wiley: New York, 1976. (b) Forster, P. M.; Burbank, A. R.; Livage, C.; Férey, G.; Cheetham, A. K. *Chem. Commun.* **2004**, 368.
(14) Anokhina, E. V.; Jacobson, A. J. *J. Am. Chem. Soc.* **2004**, *126*, 3044.

autoclave, and heated at 150 °C for 8 days. Increasing the temperature to 160−180 °C led to higher yields of **2** but did not result in larger crystals. Diluting the starting solution 5 times led to the formation of only $[NiAsp(H_2O)_2]\cdot H_2O$ phase.

*Study of the Transformation of **1** to **2**.* The previously reported one-dimensional compound **1**, $[Ni_2O(L\text{-}Asp)(H_2O)_2]\cdot 4H_2O$, forms at lower pH ($pH_{fin} = 5.0$) from a mixture of the same reagents with a $NiCl_2$:H_2Asp:Et_3N molar ratio of 1:0.5:1.25. While this mixture has a much higher Ni^{2+}:Asp^{2-} ratio than that in **2**, increasing its pH by addition of 0.25 equiv of Et_3N per Ni ($pH_{fin} = 6.1$) led to the formation of **1** and **2** in ca. 2:1 ratio, and further addition of 0.25 equiv of Et_3N per Ni ($pH_{fin} = 7.2$) led to a mixture of **2** and $Ni(OH)_2$, illustrating the effect of pH on the dimensionality of Ni−O−Ni bonding. Compound **2** also formed (as a mixture with an unidentified amorphous phase) when 0.25 equiv of Et_3N per Ni and a small amount of water were added to a sample of **1** and heated at 150 °C in a Teflon-lined autoclave. To investigate whether **2** can be obtained from **1** via a topochemical reaction of connecting the chains in **1** with $(NiAsp_2)^{2-}$ units, we added the corresponding amount of a 1 M solution of $(Et_3NH)_2(NiAsp_2)$ to a sample of **1**, and an overnight reaction at 100 °C resulted in a mixture of **2** and $[NiAsp(H_2O)_2]\cdot H_2O$. The same reaction at 50 °C, however, led to a mixture of **1** and $[NiAsp(H_2O)_2]\cdot H_2O$, suggesting that the transformation of **1** to **2** occurs through the $[NiAsp(H_2O)_2]\cdot H_2O$ intermediate.

Characterization. *Thermal Stability Studies.* Thermogravimetric analysis was carried out in air or pure oxygen at a heating rate of 1 °C/min using a high-resolution TGA 2950 thermogravimetric analyzer (TA Instruments). A study of the framework stability as a function of temperature and identification of the decomposition products were performed by X-ray powder diffraction.

N_2 Absorption Measurements. Nitrogen absorption isotherms were measured using a COULTIER OMNISORP 100 automated gas sorption analyzer. A sample of **2** (synthesized from a reaction mixture with a $NiCl_2$:H_2Asp:Et_3N molar ratio of 1.25:1:2.5) was dehydrated under vacuum at 80 °C overnight, and its N_2 absorption isotherm was measured for P/P_0 values up to 0.2. The total volume absorbed was ca. 67 mL/g. The pore size distribution plot showed a sharp maximum at 5.5 Å and a large fraction of the adsorbed volume corresponding to mesopores. A partial decomposition of the framework after dehydration was observed by X-ray powder diffraction. A second sample of **2** with a larger particle size (synthesized from a reaction mixture with a $NiCl_2$:H_2Asp:Et_3N molar ratio of 1:1:2) was dehydrated under vacuum at 80 °C for 24 h, and the N_2 absorption measurements indicated significantly lower absorbed volumes, even for the micropore region, suggesting either an incomplete dehydration or a higher degree of decomposition of the framework (or both). Further heating of the sample at 150 ° C for 4 h led to a negligible N_2 absorption.

Absorption of 1,3-Butanediol. A 3.00 g sample of **2** (synthesized from a reaction mixture with a $NiCl_2$:H_2Asp:Et_3N molar ratio of 1.25:1:2.5) was stirred in 10 mL of racemic 1,3-butanediol (bp 204 °C) until formation of a uniform suspension. The mixture was stirred and heated in an open container for 4 h at 180 °C. Subsequently, the mixture was centrifuged, and the solid was washed with ethanol and dried in air. The powder pattern of the resulting solid was identical to that of as-synthesized **2**, and thermogravimetric analysis indicated adsorption of ca. 19 mass % of 1,3-butanediol. No enantiomeric selectivity of this absorption was detected by optical rotation measurements of the decanted 1,3-butanediol and of a solution of the solid product in 2 M HCl.

Crystal Structure Determination. A blue thin needlelike crystal (0.010 × 0.010 × 0.24 mm) was mounted on a glass fiber, and intensity data were initially collected at 223(2) K on a Siemens SMART/CCD diffractometer using Mo Kα radiation. A hemisphere of data (1271 frames) was measured with an omega rotation of 0.3° and an exposure time of 170 s per frame. Data extraction and reduction were performed using SAINT software.[15] Indexing of all measured reflections with $I > 10\sigma(I)$ (255 reflections) gave a tetragonal unit cell with $a = 18.278(7)$ Å and $c = 11.731(6)$ Å, and the systematic absences indicated the space group $P4_12_12$, which was in agreement with the unit cell parameters and the space group determined from powder diffraction data ($a = 18.30(1)$ Å, $c = 11.717(7)$ Å). In the resulting dataset the average $I/\sigma(I)$ ratio was only 1.02 for a 2θ cutoff of 55° (0.77 Å) and 1.59 for a 2θ cutoff of 41.6° (1.00 Å), yet the direct methods structure solution with subsequent Fourier cycles (SHELXTL package[16]) revealed the positions of all nickel and coordinating oxygen and nitrogen atoms as well as of all carbon atoms of the aspartate ligand within the helices. Isotropic refinement of this partial structure model led to $R_1 = 0.18$ for 843 reflections with $I > 2\sigma(I)$. After a period of approximately 4 months, the data were collected on the same crystal using synchrotron radiation ($\lambda = 0.9223$ Å) at the X7B beamline of the National Synchrotron Light Source at Brookhaven National Lab. The data were measured using an imaging plate detector (Mar345, 2300 × 2300 pixels). Two diffraction datasets were measured at room temperature in an oscillation mode: one hemisphere by rotating the crystal in phi by 3° in 480 s per frame and the second by 6° in 60 s per frame. The intensities were integrated and merged using the DENZO program.[17] Corrections for Lorentz−polarization effects were made, and no absorption correction was applied. The average $I/\sigma(I)$ ratio for the new dataset was 12.67 (for a 2θ cutoff of 54.8° (1.00 Å)), and the positions of the remaining atoms of the aspartate ligand in the bridging unit and most of the guest water molecules could be readily located from the Fourier difference maps. The thermal displacement parameters of all atoms, however, were considerably large and, on average, by a factor of 1.8 larger than those obtained from the CCD dataset. Refinement of the structure in lower symmetry groups ($P4_1$ and $P2_12_12_1$) or using a synchrotron dataset collected at 150 K did not lead to new structural features or a significant decrease in thermal displacement parameters, suggesting that their high values are probably caused by a partial degradation of the crystal. The Flack parameter was 0.59(10), but the absolute configuration of **2** was determined unambiguously based on the presence of L-enantiomers of the aspartate ligands.

Table 1. Crystallographic Data for Compound 2

chemical formula	$C_8H_{24.10}N_2Ni_{2.5}O_{15.55}$
fw	543.97
cryst syst	tetragonal
space group	$P4_12_12$ (No. 92)
a, Å	18.186(7)
c, Å	11.706(6)
V, Å^3	3872(3)
Z	8
T, K	298(2)
ρ_c, g cm^{-3}	1.867
μ(Mo Kα), mm^{-1}	2.50
R1, wR2 [$I > 2\sigma(I)$][a]	0.0840, 0.2188
R1, wR2 (all data)[a]	0.1062, 0.2413

[a] $R1 = \Sigma||F_o| - |F_c||/\Sigma|F_o|$. $wR2 = [\Sigma w(F_o^2 - F_c^2)^2/\Sigma w(F_o^2)^2]^{1/2}$.

In the final cycles all non-hydrogen atoms except for O8, C4, C11, and C41 and the guest water molecules were refined anisotropically. The hydrogen atoms from the aspartate ligands were included in calculated positions and refined using a riding model with fixed isotropic displacement parameters. The hydrogen atom from μ_3-hydroxide ligand (OH9) was placed 1 Å from OH9 on the line connecting OH9 with the guest water molecule Ow2 (OH9−Ow2 distance is 2.944(1) Å). Only 5.28 out of 6.55 guest water molecules have been located by structure analysis. Crystallographic data for **2** based on the room-temperature synchrotron dataset are summarized in Table 1.

(15) *SAINT: Software for the CCD Detector System*; Bruker Analytical X-ray System: Madison, WI, 1995.
(16) *SHELXTL*: *Program Library for Structure Solution and Molecular Graphics*, version 5.10 (PC version); Bruker Analytical X-ray Systems: Madison, WI, 1998.
(17) Otwinowski, Z.; Minor, W. In *Methods in Enzymology*; Carter, C. W., Sweet, R. M., Eds.; Academic Press: New York, 1997; pp 307−326.

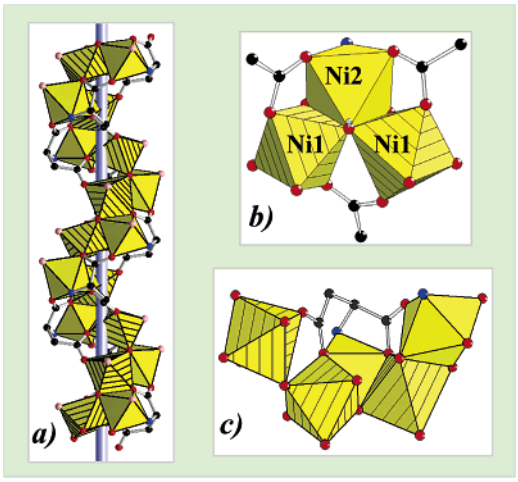

Figure 2. (a) Helical chain in one-dimensional nickel aspartate $[Ni_2O(L\text{-}Asp)(H_2O)_2]\cdot 4H_2O$ (**1**). Hatched octahedra: $Ni(1)O_5(H_2O)$. Not hatched octahedra: $Ni(2)O_4N(H_2O)$. In compound **2** the terminal aqua ligands (shown in pink) are replaced by carboxylate groups from $[Ni(3)Asp_2]^{2-}$ bridges. (b) Trimeric $Ni_3(OH)O_{12}N$ building unit in **2**. (c) Coordination of aspartate ligands within the main helix (Asp(1)) in **2**.

Magnetic Measurements. Static magnetic susceptibility of **2** as a function of temperature at 5, 100, and 20000 G and hysteresis loops at 2 and 6 K were measured using a Quantum Design SQUID magnetometer on a powder sample of **2** placed in a gel capsule.

Results and Discussion

Structure Description. The main building blocks of the three-dimensional framework of **2** (Figure 1b) are helical chains of edge- and corner-sharing Ni octahedra analogous to those in $[Ni_2O(L\text{-}Asp)(H_2O)_2]\cdot 4H_2O$[14] (**1**) (Figure 2a). The structure of **2** is derived from **1** by linking these helices with $[NiAsp_2]^{2-}$ bridges so that the terminal aqua ligands located on the periphery of the helices in **1** are replaced with carboxylic groups from the $[NiAsp_2]^{2-}$ units. The charge of the $[NiAsp_2]^{2-}$ units is balanced by substitution of μ_3-O^{2-} with μ_3-OH^- ligands. The helical chains in **2** are based on a trimeric unit $Ni_3(OH)O_{12}N$ where one $Ni(2)(OH)O_4N$ octahedron shares its two 60° adjacent edges with two $Ni(1)O_6$ octahedra (Figure 2b). The trimers link to each other via $Ni(1)O_6$ octahedra, so that in the resulting chain each $Ni(1)O_6$ octahedron shares its trans corners with two $Ni(1)O_6$ octahedra and skew edges with two $Ni(2)O_5N$ octahedra (Figure 2a). Each aspartate ligand within the helix (Asp(1)) coordinates to five nickel atoms (Figure 2c): three Ni(1) and one Ni(2) in a monodentate mode through carboxylic groups and one Ni(2) in a chelating tridentate mode through the amino group and one oxygen from each carboxylic group. The latter local tridentate chelating coordination geometry is typical in transition-metal aspartate complexes and occurs, in particular, in the polymeric chain compound $[NiAsp(H_2O)_2]\cdot H_2O$.[8a]

The additional Ni atoms (Ni(3)) are located on the 2-fold symmetry axes and coordinated by two aspartate ligands (Asp(2)) in a tridentate chelating mode so that the nitrogen atoms (N(2)) and oxygen atoms from α-carboxylic groups (O(5)) and ω-carboxylic groups (O(7)) are located in cis, trans, and cis positions with respect to the corresponding atoms of the symmetry-related aspartate ligand (Figure 3). The *trans*-O(5) atoms are shared with the $Ni(2)O_4(OH)N$ octahedra from the helices, creating an extended 3D Ni−O−Ni network, and the remaining oxygen atoms from the α-carboxylic groups (O(6)) reinforce these linkages by connecting to $Ni(1)O_5(OH)$ octahedra from the helices. Substitution of two terminal water molecules in the original helix in compound **1** by the α-carboxylate bridge is accompanied by a decrease of the O−O separation to 2.30 Å from Ow−Ow distances of 2.61 and 3.28 Å, which is allowed by somewhat flexible linkages between the nickel octahedra within the helices. The ω-carboxylic groups of the $[Ni(3)Asp_2]^{2-}$ units coordinate only to Ni(3) atoms in a monodentate mode.

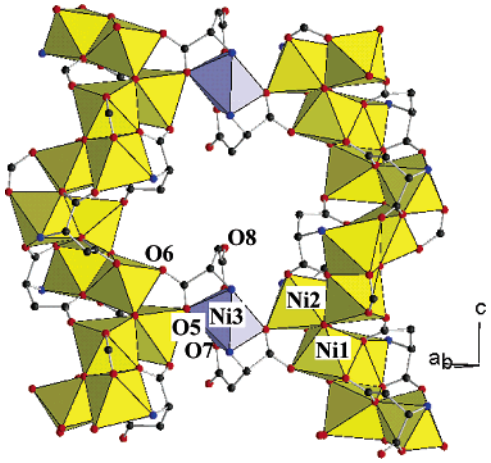

Figure 3. Fragment of structure **2** showing connectivity between the helices via $[NiAsp_2]^{2-}$ bridging units.

The linkages between the helices via the $[NiAsp_2]^{2-}$ units lead to the formation of chiral helical (symmetry 2_1) channels running parallel to the *c* axis (Figures 1 and 4). One full turn of this helix consists of 16 octahedra. The surface of the channels is lined with both hydrophobic (CH_2 and CH) and hydrophilic (OH, C═O, NH_2) groups, and their narrowest cross-section (van der Waals dimensions of ca. 5 × 8 Å) occurs where two uncoordinating carbonyl groups point in toward the channels (O(8)−O(8) distance is 7.40 Å, and the *z*-coordinates of these atoms differ by 0.86 Å) (Figure 4b). The apertures of the windows connecting the channels are less than 1.5 Å wide, even though the centers of adjacent $[NiAsp_2]^{2-}$ bridging units are separated along the *c* axis by 11.7 Å (Figure 3). The channels are filled with 6.55 water molecules per formula unit, which are disordered over 13 sites and hydrogen bonded to the hydrophilic groups and to each other.

Thermal Stability and Absorption Properties Compound **2** loses 6.55 guest water molecules in one wide step from room temperature to 275 °C (obsd 21.7%, calcd 22.0%). At 275 °C, it decomposes in one step to give a mixture of Ni and NiO (obsd 47.3%, calcd for pure NiO 43.1%, for pure Ni 51.3%). After a 4 h treatment at 150 °C, compound **2** partially loses its crystallinity, which can be restored by a 4 h treatment in water vapor at 100 °C. A 4 h treatment in racemic 1,3-butanediol at 180 °C resulted in a partial loss of water without decomposition of the framework and in a nonenantioselective adsorption of 19% of 1,3-butanediol. The N_2 adsorption isotherm of **2** shows two regions corresponding to micropores and mesopores. The total volume adsorbed for P/P_0 below 0.2 is 67 mL/g, and the BET surface area is 157 m^2/g.

Magnetic Properties. Compound **2** represents one of the few examples of a long-range magnetic ordering in homochiral compounds.[18] These compounds are of particular interest in investigation of the recently discovered phenomena associated

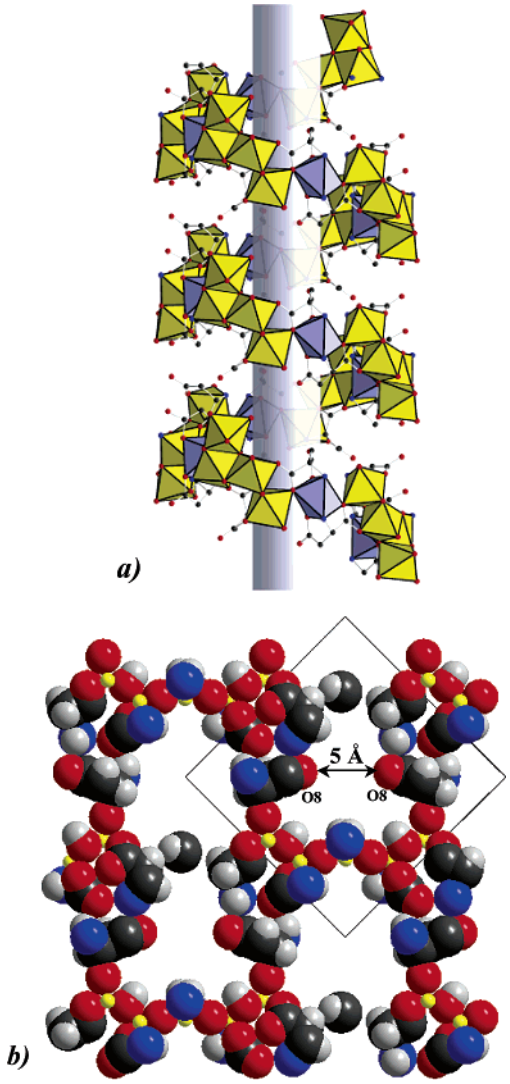

Figure 4. Channels in compound **2**: (a) view showing the helical character of the channels; (b) cross-section of the structure parallel to the *ab* plane at $z = 0.25$ showing the narrowest and widest regions of the channels. The guest water molecules are omitted for clarity (nickel, yellow; oxygen, red; nitrogen, blue; carbon, dark gray; hydrogen, light gray).

with coexistence of magnetism and optical activity.[19] Compound **2** undergoes a ferrimagnetic ordering transition ($T_c = 5.5$ K, Figure 6a) featuring a moderate hysteresis (Figure 6b). At 2 K, the coercive field is ca. 750 G and the remnant magnetization is 0.49 μ_B per nickel. The magnetization saturates at 1.3 μ_B per nickel, which is lower than the value for fully aligned spins for $S = 1$ (2 μ_B).[20] At $T = 22$ K, there is another magnetic transition without hysteresis (Figure 6c). At $T > 30$ K, the susceptibility of **2** follows Curie−Weiss law (Figure 6c) with $\theta = 4.5$ K and $\mu_{eff} = 3.06$ μ_B, which is close to the spin-only value for $S = 1$ ($\mu_{eff} = 2.83$ μ_B).

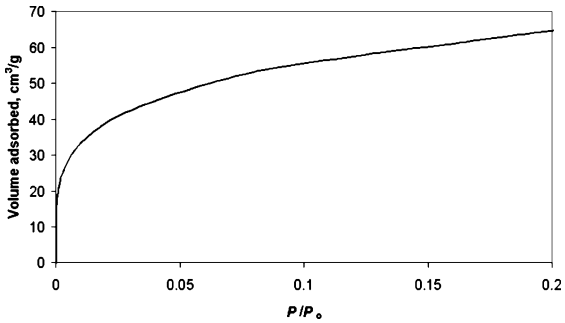

Figure 5. Nitrogen gas sorption isotherm at 77 K for compound **2** (P/P_0 is the ratio of gas pressure (P) to saturation pressure (P_0) with $P_0 = 764$ Torr).

Conclusions

The strategy of the use of optically pure bridging ligands under hydrolysis-favoring synthesis conditions has led to a new homochiral microporous nickel aspartate material $[Ni_{2.5}(OH)(L\text{-}Asp)_2]\cdot 6.55H_2O$ (**2**) featuring an extended 3D Ni−O−Ni network and 8 × 5 Å helical channels. Formation of a hybrid material with an extended 3D M−O−M connectivity has been observed, to our knowledge, in only four previously reported examples.[12a,13,21] Compound **2** is ferrimagnetic below 5.5 K, which is quite uncommon among chiral solids and demonstrates the potential of our synthetic strategy for the preparation of multifunctional materials. A particularly significant feature of **2** is that it is based on one-dimensional helical chains that were previously found in $[Ni_2O(L\text{-}Asp)(H_2O)_2]\cdot 4H_2O$ (**1**) and that **1** transforms to **2** (although not topochemically) as a result of pH increase. Given the vast variety of metal octahedra connectivity patterns found in succinates with extended M−O−M bonding,[11,13b,22] it is surprising to encounter a recurring structural motif. Formation of the helices common to **1** and **2** could be favored by the strong tendency of the aspartate ligand toward the tridentate chelating coordination mode which limits the range of orientations of its bonds to additional metal centers. We are currently investigating whether the formation of these helices is a common enough phenomenon to allow for substitution of the $[NiAsp_2]^{2-}$ bridges with larger dicarboxylic ligands to increase the channel size.

Acknowledgment. We thank Dr. Paul C. W. Chu and Andrei Baikalov, University of Houston, for magnetic measurements.

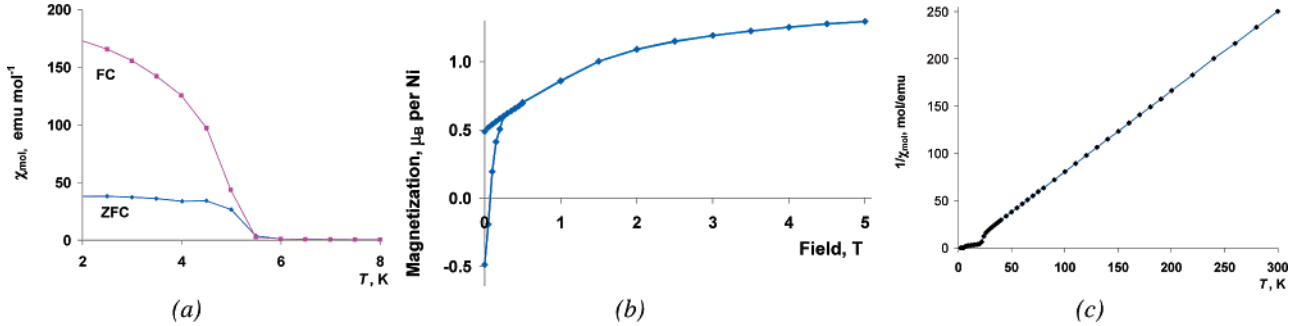

Figure 6. Magnetic properties of **2**: (a) ZFC and FC molar magnetic susceptibilities at 5 G in the temperature range 2−8 K; (b) magnetization (μ_B per Ni) as a function of applied field at 2 K; (c) inverse molar magnetic susceptibility at 100 G as a function of temperature.

This research was supported by the National Science Foundation (DMR-0120463) and the R. A. Welch Foundation. The authors thank Jonathan Hanson of the beamline X7B at the NSLS. Research carried out in part at the NSLS at BNL is supported by the U.S. DOE (DE-Ac02-98CH10886).

Supporting Information Available: IR spectrum and crystal data (CIF format). This material is available free of charge via the Internet at http://pubs.acs.org.

JA062743B

(18) For example: (a) Feyerherm, R.; Loose, A.; Ishida, T.; Nogami, T.; Kreitlow, J.; Baabe, D.; Litterst, F. J.; Sullow, S.; Klauss, H.-H.; Doll, K. *Phys. Rev. B* **2004**, *69*, 134427. (b) Armentano, D.; De Munno, G.; Lloret, F.; Palli, A. V.; Julve, M. *Inorg. Chem.* **2002**, *41*, 2007. (c) Minguet, M.; Luneau, D.; Lhotel, E.; Villar, V.; Paulsen, C.; Amabilino, D. B.; Veciana, J. *Angew. Chem., Int. Ed.* **2002**, *41*, 586. (d) Minguet, M.; Luneau, D.; Paulsen, C.; Lhotel, E.; Gorski, A.; Waluk, J.; Amabilino, D. B.; Veciana, J. *Polyhedron* **2003**, *22*, 2349. (e) Inoue, K.; Imai, H.; Ghalsasi, P. S.; Kikuchi, K.; Ohba, M.; Okawa, H.; Yakhmi, J. V. *Angew. Chem., Int. Ed.* **2001**, *40*, 4242.

(19) (a) Rikken, G. L. J. A.; Raupach, E. *Nature* **1997**, *390*, 493. (b) Andres, R.; Brissard, M.; Gruselle, M.; Train, C.; Vaissermann, J.; Malezieux, B.; Jamet, J.-P.; Verdaguer, M. *Inorg. Chem.* **2001**, *40*, 4633.

(20) Laligant, Y.; Calage, Y.; Heger, G.; Pannetier, J.; Férey, G. *J. Solid State Chem.* **1989**, *78*, 66−77.

(21) (a) Vaidhyanathan, R.; Natarajan, S.; Rao, C. N. R. *Dalton Trans*, **2003**, 1459. (b) Dybtsev, D. N.; Chun, H.; Yoon, S. H.; Kim, D.; Kim, K. *J. Am. Chem. Soc.* **2004,** *126*, 32.

(22) (a) Guillou, N.; Livage, C.; van Beek, W.; Noguès, M.; Férey, G. *Angew. Chem., Int. Ed.* **2003**, *42*, 644. (b) Livage, C.; Egger, C.; Noguès, M.; Férey, G. *J. Mater. Chem.* **1998**, *8*, 2743.